Renewable fluid dynamic energy derived from aquatic animal locomotion

2007 Bioinspir. Biomim. 2 L1

(http://iopscience.iop.org/1748-3190/2/3/L01)

IOP Publishing — Bioinspiration & Biomimetics
Bioinsp. Biomim. **2** (2007) L1–L3 doi:10.1088/1748-3182/2/3/L01

COMMUNICATION

Renewable fluid dynamic energy derived from aquatic animal locomotion

John O Dabiri

Graduate Aeronautical Laboratories and Bioengineering, California Institute of Technology, Pasadena 91125, CA, USA

Received 16 January 2007
Accepted for publication 15 August 2007
Published 10 September 2007
Online at stacks.iop.org/BB/2/L1

Abstract
Aquatic animals swimming in isolation and in groups are known to extract energy from the vortices in environmental flows, significantly reducing muscle activity required for locomotion. A model for the vortex dynamics associated with this phenomenon is developed, showing that the energy extraction mechanism can be described by simple criteria governing the kinematics of the vortices relative to the body in the flow. In this way, we need not make direct appeal to the fluid dynamics, which can be more difficult to evaluate than the kinematics. Examples of these principles as exhibited in swimming fish and existing energy conversion devices are described. A benefit of the developed framework is that the potentially infinite-dimensional parameter space of the fluid–structure interaction is reduced to a maximum of eight combinations of three parameters. The model may potentially aid in the design and evaluation of unsteady aero- and hydrodynamic energy conversion systems that surpass the Betz efficiency limit of steady fluid dynamic energy conversion systems.

Environmental flows are dominated by fluid vortices, rotating currents that vary in size from hurricanes and typhoons to the small-scale eddies created due to turbulence. It is well known that the kinematic properties of such vortices can be manipulated during interaction with a solid body, causing the kinetic energy of the incident vortices to change. Indeed, a variety of empirical and numerical studies, e.g. [2–7], have aimed to use solid objects in a flow to affect the energy of incident vortices. The goal of these studies is usually to understand the mechanism of induced drag reduction during animal locomotion or to identify the principles governing locomotion in groups (e.g., schooling fish [8, 9]). What is not clear in the existing literature is whether one can identify a simple analytical paradigm for predicting the effectiveness of a given fluid–structure interaction in terms of the vortex energy manipulation that is achieved, especially given the large parameter space that is potentially encompassed by the properties of the vortex and the solid body during fluid–structure interactions. Such a model will potentially aid not only the understanding of biological locomotion but also the design of a new class of biomimetic aero- and hydrodynamic energy conversion systems, such as a platform that was recently demonstrated [6, 7]. In this communication, we consider the properties of a model vortex-body system in order to develop a practical method of evaluating the effectiveness of vortex-based energy extraction mechanisms.

The governing model employs several simplifications. First, we will consider a cross section of a three-dimensional vortex flow in which the flow is assumed to be locally two dimensional. Hence, where the analysis considers an isolated vortex, one must imagine that it represents one section of a vortex loop, in order to satisfy Helmholtz conditions. Second, the centroid of the vortex loop propagates at a nominal speed $U = U_\infty + U_V$ along the $\mathbf{e_1}$ axis (figure 1), where U_∞ is the freestream speed. Third, to avoid the complication of infinite energy in the ambient fluid—since by assumption the fluid possesses an infinite volume and finite speed U_∞—we will conduct the analysis in the frame of reference of the freestream fluid. In the present model flow this can be accomplished by a straightforward Galilean transformation of a reference frame using U_∞ as the characteristic speed. Finally, viscous effects are neglected. These assumptions, although numerous, enable deduction of the sought after principles governing vortex

Table 1. Classification of incident vortex loop input parameters, the corresponding vortex loop energy and energy extraction protocol. The rows indicated in bold indicate the class of vortices comprising the von Karman street, the subject of recent animal and mechanical studies, e.g. [3–7].

Input parameters			Output parameters	
Rotational orientation	$\mathbf{x_{core}} \cdot \mathbf{e_2}$	$\mathbf{U_V} \cdot \mathbf{e}_1$	Incident vortex energy	Energy extraction protocol
Clockwise	Positive	Positive	Negative	Increase R
Clockwise	**Positive**	**Negative**	**Positive**	**Decrease *R***
Clockwise	Negative	Positive	Positive	Decrease R
Clockwise	Negative	Negative	Negative	Increase R
Counter-clockwise	Positive	Positive	Positive	Decrease R
Counter-clockwise	Positive	Negative	Negative	Increase R
Counter-clockwise	Negative	Positive	Negative	Increase R
Counter-clockwise	**Negative**	**Negative**	**Positive**	**Decrease *R***

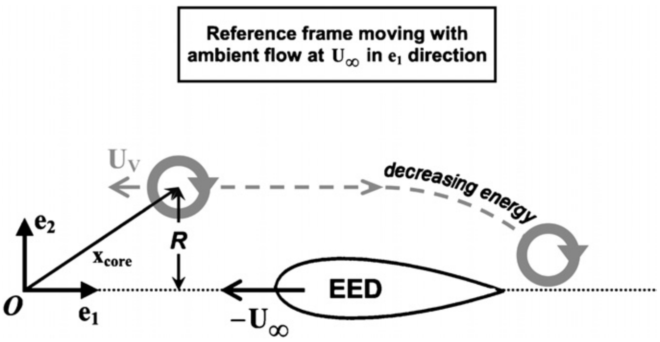

Figure 1. Kinematic parameters relevant to the model flow. An example extraction protocol (row 2 of table 1) is illustrated in the motion of the grey vortex loop cross section with clockwise circulation. EED is stationary in the laboratory frame of reference. The $\mathbf{e_3}$ coordinate direction is oriented normal to the plane of the page. ***O***, origin.

energy extraction while simplifying the problem to the point that it is analytically tractable.

Given the aforementioned model assumptions, the energy content E_V (per unit fluid density) of the vortex loop is given by [1]

$$E_V = 2\mathbf{U_V} \cdot \mathbf{I_V} + \int_{V_V} \tilde{\mathbf{u}} \cdot (\mathbf{x} \times \boldsymbol{\omega})\, \mathrm{d}V. \quad (1)$$

The vector $\mathbf{U_V}$ is the bulk propagational velocity of the vortex relative to the ambient fluid. This velocity arises due to motion induced by adjacent segments of the vortex loop (i.e., self-propagation) and due to inviscid interaction with other vortices or the image vorticity of solid bodies in the flow. The vector $\tilde{\mathbf{u}}$ is the local velocity field induced by the vortex loop and $\mathbf{I_V}$ is the vortex momentum (i.e., impulse per unit fluid density), defined in three dimensions as

$$\mathrm{I_V} = \frac{1}{2} \int_{V_V} \mathbf{x} \times \boldsymbol{\omega}\, \mathrm{dV}. \quad (2)$$

The position vector $\mathbf{x}$ is measured relative to the origin ***O*** of the coordinate system ($\mathbf{e_1}$, $\mathbf{e_2}$, $\mathbf{e_3}$); see figure 1. Finally, V_V is the region occupied by the vortex loop containing a vorticity distribution $\boldsymbol{\omega}$. In the present context it will be sufficient to assume that V_V coincides with the region of the flow containing non-zero vorticity.

Dimensional analysis of equation (1) indicates that the magnitude of the vortex kinetic energy scales as $E_V \sim \pm R\Gamma^2$, where the parameter R is the average moment arm of the vorticity distribution in the vortex loop and Γ is the circulation of the vortex loop. For the model configuration in figure 1, the parameter R can be estimated by projecting the loop-averaged vortex core position $\overline{\mathbf{x_{core}}}$ onto the $\mathbf{e_2}$ axis, i.e. $R = |\overline{\mathbf{x_{core}}} \cdot \mathbf{e_2}|$, since by assumption the centroid of the vortex loop propagates along the $\mathbf{e_1}$ axis. The sign of the vortex energy E_V indicates the magnitude of the combined freestream-vortex system energy relative to the freestream alone; negative values of vortex energy indicate that the energy of the combined freestream-vortex system is less than that of the freestream alone, and vice versa. In the absence of other vortices or bodies in the flow, E_V is always greater than zero since the vortex velocity is entirely due to self-propagation and therefore shares the same orientation as the vortex impulse (i.e., $\mathbf{U_V} \cdot \mathbf{I_V} > 0$). However, if the presence of other vortices or solid bodies in the flow dominates the vortex motion such that the vortex velocity and impulse (as defined in equation (2)) are oriented in opposite directions, then negative values of E_V can arise.

In practice, the energy of the model vortex loop can be evaluated by examining three parameters: (1) the rotational orientation of any cross section of the loop; (2) the location of that cross section above or below the origin (i.e., the local sign of $\mathbf{x_{core}} \cdot \mathbf{e_2}$), and (3) the direction of vortex loop propagation (i.e., the sign of $\mathbf{U_V} \cdot \mathbf{e}_1$). For example, if a cross section of the vortex loop possesses a counter-clockwise circulation and is located above the $\mathbf{e_1}$ axis, then the kinetic energy of the vortex loop is positive if it moves in the positive-$\mathbf{e_1}$ direction (i.e., $E_V \sim \mathbf{U_V} \cdot (\mathbf{x} \times \boldsymbol{\omega})_\mathbf{V} > 0$) and negative if it moves in the negative-$\mathbf{e_1}$. Table 1 lists all eight possible combinations of these parameters, and the resulting sign of the incident vortex loop energy.

Now, let us immerse a solid object in the fluid such that it is oriented against the flow direction and parallel to the $\mathbf{e_1}$ axis (figure 1). Due to the aforementioned inviscid assumption, the object (henceforth called the energy extraction device, or EED) only interacts with the incident vortex via its imposed pressure field or its image vorticity distribution. Note that if the EED is stationary in the laboratory reference frame, then it moves at $-\mathbf{U}_\infty$ in the reference frame moving with the freestream flow. Implicit in the relationships between vortex kinematics and vortex energetics in table 1 is a set of vortex manipulations—based solely on the loop-averaged vorticity moment arm R—by which the energy of vortices incident on the EED can be reduced to a new, lower energy spatial configuration during their interaction with the EED. Specifically, the vorticity moment arm R should be increased for incident vortices with negative energy (i.e., energy of the freestream-vortex system less than that of the freestream alone), in order to cause the vortex energy to become further reduced (i.e., a larger negative value). Conversely, the energy of incident vortices with $E_V > 0$ is reduced by decreasing the parameter R during the interaction with the EED. Since the total kinetic energy of the model system (vortex loop and EED) is conserved—and is finite due to our choice of the reference frame—kinetic energy lost by the vortex loop is gained by the EED. The mechanical energy transferred to the EED can potentially be converted to more useful forms (e.g., electricity) for immediate use or storage.

One might infer from the proposed framework the need for the EED to actively 'sort' incident vortices according to their classification in table 1, a cumbersome if not unrealistic prospect. However, recent empirical evidence demonstrates that this is unnecessary. Euthanized fish are capable of exhibiting the energy extraction protocol proposed here [5]. To do so, the animals must be artificially oriented to face upstream in the direction of the incident vortices. However, after this initialization the subsequent vortex-based energy extraction is achieved by wholly passive mechanisms as long as interactions with the source of incident vortices (an upstream bluff body) are avoided. Flow visualizations of biological fluid–structure interactions [3–5, 8, 9] and others using mechanical devices [2, 6] indicate (albeit indirectly and/or anecdotally, e.g. J C Liao personal communication) that subsequent to the interaction with the solid body the vortices can indeed be observed to take a new spatial configuration that appears consistent with the paradigm for vortex energy extraction outlined in table 1. The slaloming von Karman gait associated with fish (live or euthanized) exploiting vortices [3–5, 8, 9] may be a manifestation of these energy extraction protocols, when viewed in the appropriate frame of reference (cf table 1, rows in bold).

The viscosity and three dimensionality of real fluid flows suggest that in order for the coherence of the incident vortices to be preserved, their manipulation by the EED must occur primarily by inviscid mechanisms, e.g. the pressure field applied by the EED on the incident vortex. Viscous forces or shear effects (e.g., vortex formation and stretching) that do occur may cause the incident vortices to take on a less organized, possibly chaotic, structure after interaction with the ECD. These dissipative effects are not included in the vortex energy extraction protocols of table 1. Notwithstanding, the fact that the protocols derived from the model vortex system seem to be observed in real animals [3–5, 8, 9] suggests that the model simplifications are reasonable.

One reason the simple vortex model is able to predict the empirical observations is that the model is based on the propagation of a vortex loop. These loops are commonly observed in bluff body flows due to the constraint the Helmholtz law places on the connectivity of vortex lines in a flow [1]. The vortex wake created by a bluff body upstream of an animal [3–5, 8, 9] and the vorticity generated at the head of a swimming animal [10] will tend to form vortex loops with a well-defined moment arm that can be manipulated according to the strategy derived from the model vortex ring flow.

Biomimetic devices achieving vortex energy extraction and storage have been developed and tested in recent years [6, 7]. The impetus for these vortex-based energy conversion devices comes in part from the Betz limit that constrains the maximum fluid dynamic efficiency of traditional steady flow energy conversion systems (e.g., windmills) to 59.3% [11]. Since devices operating near this limit have now been achieved, further improvements in performance may require a shift in paradigm to systems that utilize the inherent unsteadiness of environmental flows. The framework described here can facilitate the design and evaluation of future unsteady vortex-based systems that can exceed the Betz limit.

References

[1] Saffman P G 1992 *Vortex Dynamics* (Cambridge: Cambridge University Press)

[2] Gopalkrishnan R, Triantafyllou M S, Triantafyllou G S and Barrett D 1994 Active vorticity control in a shear-flow using a flapping foil *J. Fluid Mech.* **274** 1–21

[3] Liao J C, Beal D N, Lauder G V and Triantafyllou M S 2003 The Karman gait: novel body kinematics of rainbow trout swimming in a vortex street *J. Exp. Biol.* **206** 1059–73

[4] Liao J C, Beal D N, Lauder G V and Triantafyllou M S 2003 Fish exploiting vortices decrease muscle activity *Science* **302** 1566–9

[5] Beal D N, Hover F S, Triantafyllou M S, Liao J C and Lauder G V 2006 Passive propulsion in vortex wakes *J. Fluid Mech.* **549** 385–402

[6] Allen J J and Smits A J 2001 Energy harvesting eel *J. Fluids Struct.* **15** 629–40

[7] Taylor G W, Burns J R, Kammann S M, Powers W B and Welsh T R 2001 The energy harvesting eel: a small subsurface ocean/river power generator *IEEE J. Ocean. Eng.* **26** 539–47

[8] Breder C M 1965 Vortices and fish schools *Zoologica* **50** 97–114

[9] Weihs D 1973 Hydromechanics of fish schooling *Nature* **241** 290–1

[10] Hanke W and Bleckmann H 2004 The hydrodynamic trails of Lepomis gibbosus (Centrarchidae), Colomesus psittacus (Tetraodontidae) and Thysochromis ansorgii (Cichlidae) investigated with scanning particle image velocimetry *J. Exp. Biol.* **207** 1585–96

[11] Betz A 1926 *Wind-energie und Ihre Ausnutzung durch Windmühlen* (Vandenhoeck: Ruprecht Göttingen)